Progress in development of the neutron profile monitor for the large helical device

journal or publication title	Review of Scientific Instruments
volume	85
page range	11E110
year	2014-11
NAIS	8681
URL	http://hdl.handle.net/10655/00013082

Progress in Development of the Neutron Profile Monitor for the Large Helical Device[a)]

K. Ogawa,[1,b)] M. Isobe,[1,2] E. Takada,[3] Y. Uchida,[3] K. Ochiai,[4] H. Tomita,[5] A. Uritani,[5] T. Kobuchi,[1] and Y. Takeiri[1,2]

[1]National Institute for Fusion Science, Toki, 509-5292, Japan

[2]The Graduate University for Advanced Studies (SOKENDAI), Toki, 509-5292, Japan

[3]Toyama National College of Technology, 13 Hongo-machi, Toyama, 939-8630, Japan

[4]Fusion Research and Development Directorate, Japan Atomic Energy Agency, Tokai, Naka, Ibaraki, 319-1195, Japan

[5]Nagoya University, Furo-cho, Chikusa-ku, Nagoya, 464-8603, Japan

The neutron profile monitor stably operated at a high-count-rate for deuterium operations in the Large Helical Device has been developed to enhance the research on the fast-ion confinement. It is composed of a multichannel collimator, scintillation-detectors, and a field programmable gate array circuit. The entire neutron detector system was tested using an accelerator-based neutron generator. This system stably acquires the pulse data without any data loss at high-count-rate conditions up to 8×10^5 counts per second.

I. INTRODUCTION

Neutron diagnostics have been used to study the properties of a magnetic confined fusion plasma. Neutron profile monitor (NPM) composed of a multichannel collimator and scintillation detectors has been working to measure a neutron emission profile at large tokamaks, such as the Tokamak Fusion Test Reactor,[1,2] the Joint European Torus,[3-5] and JT-60 Upgrade,[6] and will be installed in ITER.[7,8] The NPM provides valuable information, such as energetic ion confinement, neutron yields, and neutral beam deposition. The effect of magnetohydrodynamic instabilities such as sawteeth,[3] and an abrupt large-amplitude event[9] on energetic ion confinement has been revealed by the NPM. The Large Helical Device (LHD) has been working successfully for 16 years using a hydrogen gas. To achieve higher performance plasmas, operations with a deuterium gas and deuterium beams on the LHD will start in a few years. In deuterium experiments, the neutrons are mainly produced by the beam-plasma reaction. Thus, further progress in the study of a fast-ion confinement is possible. Installation of NPM was planned in the second phase of LHD experiment e.g. deuterium plasma experiments from the early stage.[10] And then, a conceptional design, such as installation location and a preliminary calculation of the multichannel collimator design was reported.[11] In this paper, we will describe the progress in development of the NPM.

II. NEUTRON PROFILE MONITOR FOR THE LHD

The NPM will be installed on the basement level of the LHD building and the plasma will be seen from the lower side as shown in Fig. 1. The NPM consists of three parts: a multichannel collimator, an eleven-scintillation-detector (a scintillation material coupled with a photomuliplier), and a digital-based data acquisition system.
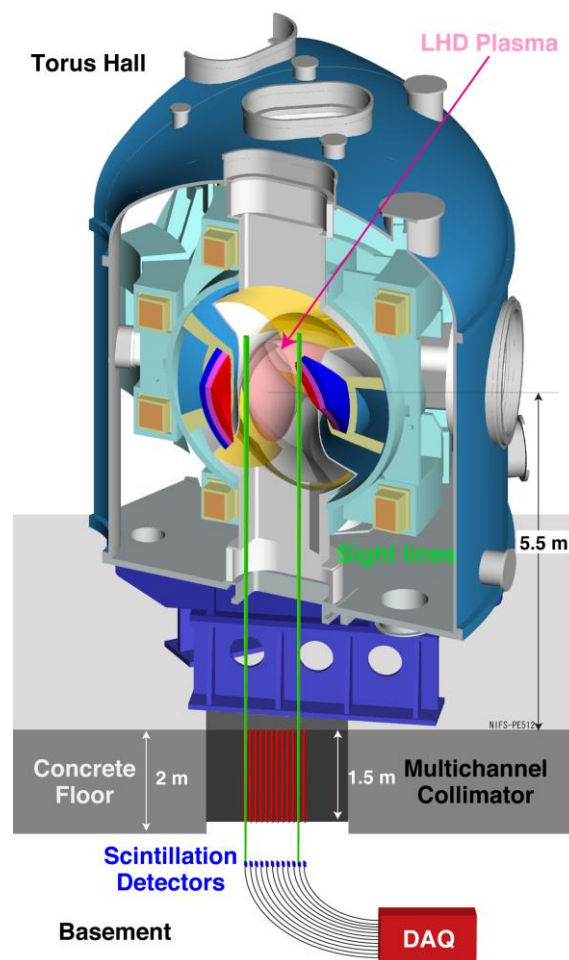

Fig.1 Schematic view of NPM for the LHD.

A. The Multichannel Collimator

The multichannel collimator will be installed in the concrete floor of the LHD. A possible space for the collimator is 800 mm x 1400 mm and 2.0 m in height. We will make 11 sight lines aligned radially: a diameter ϕ of each hole is 30 mm and the distance between the centers of two holes is 90 mm. Note that ϕ of the hole can be changed from 10 mm to 30 mm by means of stainless pipes. We compared the performance of a collimator made of pure-polyethylene (1.5 meters in thickness) plus lead (0.15 meters in thickness) and one made of a heavy concrete (1.5 meters in thickness) by means of the MCNP code.[12] In this calculation, we simulate the LHD plasma as a 2.45 MeV neutron source. Here the heavy concrete is Colemanite ($CaB_3O_4(OH)_3 \cdot H_2O$) and hematite ($Fe_2O_3$)-doped concrete whose density is about 3.5 g/cm³. Colemanite is doped for capturing thermal neutrons, whereas for attenuating gamma rays hematite is doped. Figures 2 a) and b) show neutrons and gamma ray spectra at a detector position by the calculation. It shows that a polyethylene plus lead and heavy concrete have a similar neutron and gamma ray shielding performance. Note that in the case of polyethylene plus lead, we can observe 2.2 MeV gamma rays produced by an H(n,γ)D reaction. This means that some gamma rays can directly come from a polyethylene to the detector through the hole in the lead. We will choose a collimator made of a heavy concrete because of two reasons. One is that it has superior performance in reducing unwanted gamma rays directly coming to a detector compared with one made of polyethylene plus lead. The other is that it is relatively easy to make a multichannel collimator using heavy concrete (it is difficult to lay polyethylene and lead bricks precisely inside the limited space).
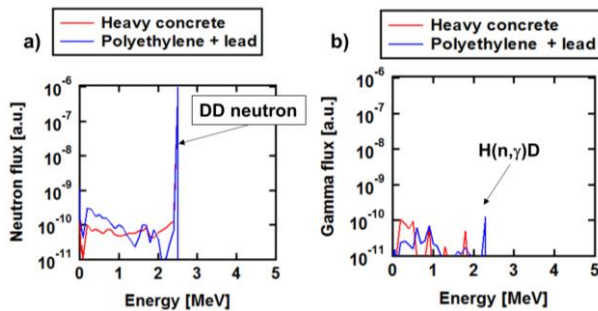

Fig.2. Energy spectrum of neutron and gamma ray reaching to the scintillation detector.

B. Scintillation Detectors

We tested three pulse-shape-discrimination (PSD) scintillation materials, stilbene, NE213, and EJ299-33, in comparing their performance. Note that the size of the scintillation materials is the same: ϕ of 20 mm and height of 10 mm. Each scintillation material is coupled with a photomultiplier tube (H11934-MOD: HAMAMATSU Photonics which has high-gain stability). We compared the brightness and the PSD ability of each scintillator by using ^{137}Cs and ^{252}Cf sources, respectively, as shown in Fig. 3 a). In experiments, an analysis of pulse signals is done by using DT5751 with digital pulse processing for the PSD software made by CAEN. Width of pulses is almost the same among three scintillation detectors, therefore, we can compare the total charge of one pulse (Q_{long}) of the Compton edge to find the brightest scintillation materials. A spectrogram of Q_{long} is plotted in Fig. 3 b). Stilbene and EJ299-33 are about one order brighter than NE213. This result is incongruous with Ref.

13, according to which the brightness of an NE213 material is the same order as that of a stilbene. It may be possible to induce this difference which is a collection efficiency of a scintillation light by a photomultiplier. NE213 material is filled in a glass box. The light generated by radiation in NE213 material may fly in any direction. Photomultiplier can collect photons directly coming from a NE213 material. On the other hand, a stilbene is a white-coated solid material with the photomultiplier side polished. The white coating can reflect the light generated in a stilbene material. Photomultiplier can collect not only photons directly coming from a stilbene material but also photons reflected by the white coating. Figure 3 c) shows the typical neutrons and gamma rays discrimination map. In this plot, a shaping parameter (SP) is $(Q_{long} - Q_{short})/Q_{long}$. Here, Q_{long} and Q_{short} are total charge of one pulse and its short component (integrated in t_{short} bin), respectively. Note that typical t_{short} for the stilbene detector and the NE213 detector are 11 ns and 14 ns, respectively. Note that it is impossible to discriminate pulse shape using EJ299-33 scintillation material in this experiment because SPs of neutron and gamma ray pulse are almost the same. Table 1 shows the summary of the brightness and the Figure of Merit (FOM) for three scintillation detectors. Stilbene is the best for an NPM because of a higher brightness and a higher PSD ability. It is important to note that the stilbene has directivity of measuring neutrons and gamma rays. In our situation, our heavy concrete collimator can eliminate the neutrons coming from the side of the scintillator, thus this effect is neglectable.
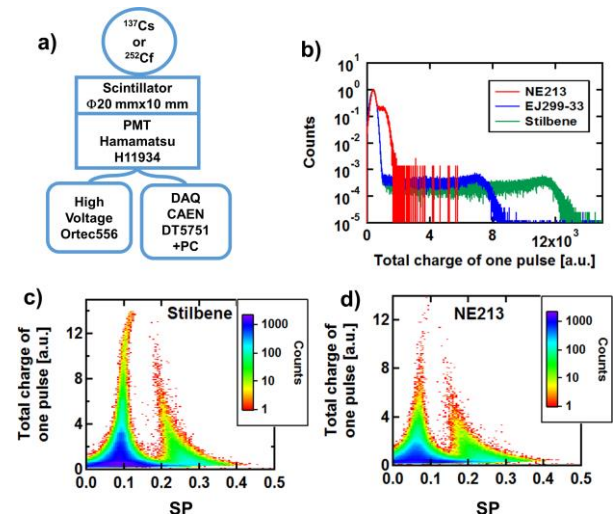

Fig.3 a) Experimental setup for evaluating performance of scintillation materials. b) Spectrogram of a total charge of one pulse of three scintillation materials. Typical result of neutron and gamma-ray discrimination of c) Stilbene and d) NE213.

Table 1 The brightness and the Figure of Merit of three scintillation materials

Scintillator	Stilbene	NE213	EJ299-33
Brightness (^{137}Cs)	11	1	7
FOM (^{252}Cf)	1.47	1.22	less than one (not discriminate)

C. Digital-based Data Acquisition System

To discriminate a pulse shape online or offline at the high-count-rate condition, a field programmable gate array (FPGA) circuit (NI5772+PXIe-7962R: National Instruments) has been developed. NI5772 is a 12 bit and wideband analog to digital

converter capable of inputs as high as 2.2 GHz at sample rates up to 1.6 GHz. PXIe-7962 is the FPGA module equipped with a Virtex-5 and a 512 MB DDR2 memory. An FPGA clock and a maximum data transfer rate are 400 MHz and 800 MB/s, respectively. For online discrimination, we adopt the charge integral method with two components as shown in Sec 2B. For offline analysis, a number of acquiring points per pulse is set to be 96 points (numbers of points for pre-trigger and post-trigger are 16 points and 80 points, respectively). The programming is done by LABVIEW 2013. Out test with pulse generator shows that with online analysis, it can acquire the data with 10 MHz rate without any data loss.

III. TEST IN ACCELERATOR-BASED NEUTRON GENERATOR

We tested the entire stilbene detector system with capability of online PSD by an FPGA circuit using an accelerator-based neutron generator on the Fusion Neutronics Source in the Japan Atomic Energy Agency. Figure 4 a) shows the setup of the experiments. DD neutrons are generated due to deuterium beams and a deuterium target reactions. We changed a beam current to change the neutron flux discretely. Note that a neutron flux rate at the detector position is up to ~2.5×10^7 cm^{-2}s^{-1}. Figure 4 b) shows the typical signal induced by the neutron and the gamma ray acquired by an oscilloscope (Tektronix DPO7104: 1 GHz bandwidth and 20 GHz sample rate). The tail of a neutron signal is longer than that of a gamma ray. The result of a neutron and gamma ray discrimination is shown in Fig. 4 c). Pulses induced by neutrons and gamma rays are clearly separated. Here, we can see several points on the right side of the plot; they are due to the pile-up of pulses. The number of these points increases with an increase of the neutron fluence rate and is the similar to the pile-up expected by simple calculation ($n/(1-n\tau)$-n: n and τ represent a count rate of pulses acquired by ADC and a total width of a pulse, respectively). It is important to note that a gain shift of the photomultiplier is not observed in the case of a count rate of 1.2×10^6 cps; a neutron-gamma ray discrimination map does not change. The acquired count as a function of a neutron flux is shown in Fig. 4 d). The pulse acquired by ADC per second increases linearly with a neutron fluence rate in the neutron

fluence rate range up to ~1.7×10^7 cm^{-2}/s: an expected count rate is ~8×10^5 cps. A counting loss is observed when the count rate exceeds 8×10^5 cps. It is due to the re-arm time of the trigger: expected to be ~60 ns. In our previous test with pulse generator, pulses came periodically, so the time difference between pulses was 100 ns when the pulse rate became 10 MHz. However, the real situation, pulses come randomly, thus such ~60 ns re-arm time can induce the data losses. We will improve our routine to acquire the data with 10^6 cps.

IV. SUMMARY

We developed a neutron profile monitor for LHD deuterium experiments. We will use the multichannel collimator made of a heavy concrete having high performance to reduce unwanted-neutrons and gamma rays. A stilbene is used as a fast-neutron scintillator because it has a higher pulse-shape-discrimination ability and a brighter light emission. The scintillation material is coupled with a photomultiplier having a high-gain stability. The signal of a photomultiplier is analyzed online or offline based on an FPGA. Test the entire system with a neutron generator shows that this system can acquire the pulses without any data loss up to 8×10^5 cps with online analysis. This system will be installed to measure the neutron profile in a LHD plasma with a high-time response.
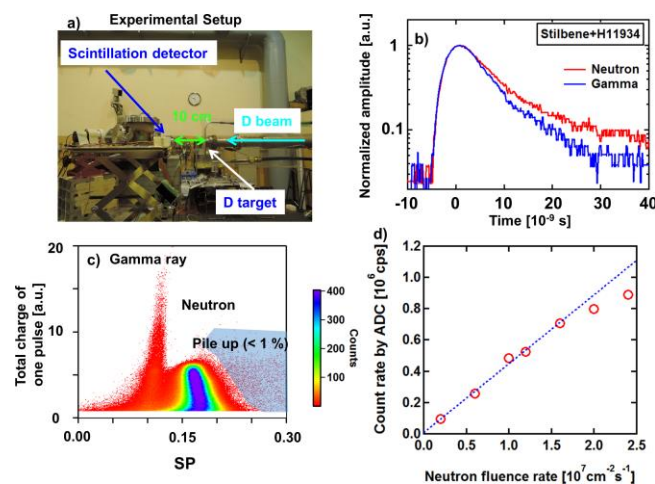
ACKNOWLEDGEMENTS

Fig.4 a) Experimental setup for testing entire system on Fusion Neutronics Source. b) Typical pulse due to neutron and gamma ray acquired by oscilloscope. c) On-line neutron-gamma discrimination in DD neutron generator. d) Count rate by ADC as a function of neutron fluence rate at detector position.

[1] A. L. Roquemore et al., Rev. Sci. Instrum. **61** 3163 (1990).
[2] A. L. Roquemore et al., Rev. Sci. Instrum. **68** 544 (1997).
[3] M. Adams et al., Nucl. Instrum. Meth. A **329** 277 (1993).
[4] O. N. Javis et al., Fusion Eng. Des. **34-35** 55 (1997).
[5] M. Riva et al., Fusion Eng. Des. **86** 1191 (2011).
[6] M. Ishikawa et al., Rev. Sci. Instrum. **73** 4237 (2002).
[7] L. Giacomelli et al., Nucl. Fusion **45** 1191 (2005).
[8] D. Marocco et al., J. Instrum. **7** C03033 (2012).
[9] M. Ishikawa et al., Nucl. Fusion, **45** 12 (2005).
[10] M. Sasao et al., Fusion Eng. Des. **34-35** 595 (1997).
[11] M. Isobe et al., Rev. Sci. Instrum. **81** 10D310 (2010).
[12] X-5 Monte Carlo Team, "MCNP - A General N-Particle Transport Code, Version 5, Volume I: Overview and Theory," Los Alamos National Laboratory, LA-UR-03-1987 (2003).
[13] G.F. Knoll, Radiation Detection and Measurement, 4th Ed. (Wiley, New York, 1999) 230.